Reprinted from JOURNAL OF THE OPTICAL SOCIETY OF AMERICA, Vol. 58, No. 8, 1133–1145, August 1968
Printed in U. S. A.

Model for Visual Luminance Discrimination and Flicker Detection

GEORGE SPERLING* AND MAN MOHAN SONDHI
Bell Telephone Laboratories, Incorporated, Murray Hill, New Jersey 07974
(Revision received 23 December 1967)

A model for vision is proposed. Its basic units are RC stages whose time constants—in three instances—are parametrically controlled. The requirements of compressing the dynamic range of the input and of fitting luminance pulse-detection data suffice to determine the arrangement and parameters of the components. This model accurately predicts the psychophysical results of flicker detection (DeLange characteristics at above 10 Hz), the Ferry–Porter and Weber laws in the ranges where they apply, the effects of light adaptation, and it accounts for individual differences. By considering the variable RC stage as an approximate analog of a synaptic excitatory process which is controlled by inhibition, significant correspondences are observed between the internal connectivity of the model and the neural connectivity of the retina.

INDEX HEADINGS; Vision; Detection.

THIS is a report on a model which attempts to account for data from psychophysical experiments in terms of an electrical network. The basic building block of the model is an RC stage whose time constant may be controlled parametrically by feedback or by feedforward. The analogy between an RC stage of variable time constant and a synaptic inhibitory process was proposed by Fatt and Katz[1] for the neuromuscular junction (motor end-plate) of crustacea and subsequently proved for mammalian motor neurons by Coombs, Eccles, and Fatt in 1955.[2] Fuortes and Hodgkin[3] suggested an electrical network of this general type to account for the transduction of light into neural signals in the eye of *Limulus*. To fit the data of various specimens, their model required 7 to 14 RC stages, each of whose time constants was controlled parametrically by feedback. No anatomical correspondence could be found for such a large number of parameter-controlled RC stages and attempts were made to derive this kind of response from totally different principles.[4]

The model proposed here to account for human photopic vision is actually simpler than Fuortes and Hodgkin's *Limulus* model, in the sense that the human

* This revision was prepared while the first author was a visiting faculty member at the University of California, Los Angeles, California.

[1] P. Fatt and B. Katz, J. Physiol. (London) **121**, 374 (1953).

[2] J. S. Coombs, J. C. Eccles, and P. Fatt, J. Physiol. (London) **130**, 396 (1955).

[3] M. G. F. Fuortes and A. L. Hodgkin, J. Physiol. (London) **172**, 239 (1964).

[4] J. Levinson, J. Opt. Soc. Am. **56**, 95/529E (1966).

model requires only three parameter-controlled stages. The model has the added advantage that its major components are compatible with what is already known about synaptic processes and about retinal connectivity.

The model may be summarized briefly as follows. The input signal is a retinal illumination which, in general, varies as a function of time. The signal passes in sequence through four main components: a 2-stage filter (FB) whose time constants τ_F are controlled by parametric feedback, a feedforward filter (FF) whose time constant τ_F is controlled by its input, 6 linear low-pass RC stages (LP), and a threshold detector (D) whose output is a signal of value 0 or 1 corresponding to nondetection or detection of the particular input signal. These components are defined explicitly below. Then, their joint action is described and applied to prediction of psychophysical experiments. Finally, their relation to retinal structure and function is considered.

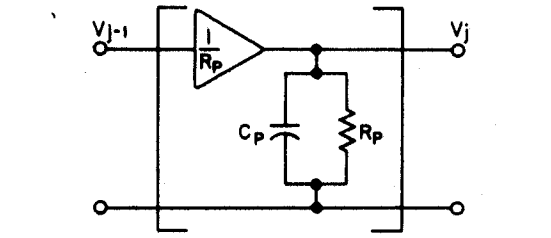

(a)

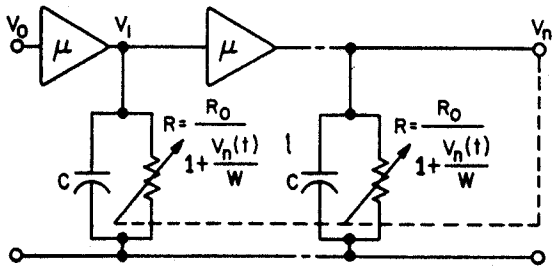

(b)

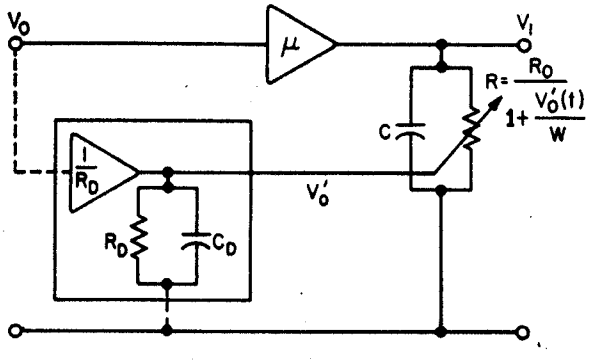

FIG. 1(a). LP stage. Electrical analog of a low-pass-filter stage. The time constant $\tau_p = R_pC_p$. The triangle here and in each of the figures indicates an isolating transconductance μ which produces an output current equal to μ times the input voltage V_{j-1}. The inscribed symbol is the value of μ. (b). FB filter. Electrical analog of an n stage parameter-controlled feedback filter (only the first and last stages are indicated). The last stage controls R of each stage as indicated. The time constant of each stage is $\tau = RC$; when the output is zero (e.g., in the dark), the time constant of each stage is $\tau = \tau_F = R_0C$. The value of μ is $1/R_0$. (c). FF filter. Electrical analog of a parameter-controlled feedforward filter with a single LP delay stage ($\tau_D = R_DC_D$) in the controlling pathway. Other symbols are defined as in (b). See text for details.

I. COMPONENTS OF THE MODEL

Low-Pass Filter, LP (Fig. 1a)

We shall use the term p-stage LP filter for a system that is governed by the equations

$$\tau_p \frac{d}{dt} v_j(t) + v_j(t) = v_{j-1}(t) \quad j = 1, \cdots, p. \tag{1}$$

In the terminology of an electrical engineer, the set of Eqs. (1) represents a cascade connection of p RC stages separated by isolation amplifiers. Here $v_0(t)$ is the input to the first stage and $v_p(t)$ the output of the final stage. The constant $\tau_p = R_pC_p$ is the time constant of each stage.

The function of the LP filter in the model is to set the upper limit on the speed of response, i.e., the limit of temporal resolution. The resolution limit is determined by τ_p and p together. The response characteristics of an LP filter are independent of the input level; it is a linear filter whose characteristics are well known.[5]

Parametric-Feedback Filter, FB (Fig. 1b)

The term FB filter is used here for a cascade connection of n RC stages, similar to the LP filter except that the output of the final stage controls the time constant τ of each of the stages. The functional dependence of the time constant τ on the output is

$$\tau = \tau_F / [1 + v_n(t)], \tag{2a}$$

where τ_F is the time constant of each stage in the absence of any input to the filter. The equations representing such a filter can be written in the form

$$\frac{d}{d\lambda} v_j(\lambda) + v_j(\lambda)[1 + v_n(\lambda)] = v_{j-1}(\lambda) \quad j = 1, \cdots, n, \tag{2b}$$

with $\lambda = t/\tau_F$. The $v_j(t)$ are dimensionless quantities chosen to permit the equations for the FB filter to be written in their simplest form. They are related to the actual voltages $V_j(t)$ of the network in Fig. 1(b) by

$$v_j(t) = (\mu R_0)^{n-j} V_j(t)/w. \tag{2c}$$

The dimensional constants w, μ, and R are needed to

[5] For a review of LP filters in relation to vision see G. Sperling, Doc. Ophthalmol. 18, 3 (1964).

establish physical units for voltage, current, and resistance, but w, μ, and R are irrelevant to the behavior of the system, and do not appear in Eqs. (2a) and(2b).[6]

Some properties which we have been able to prove for FB filters are stated here in simple terms.

Generally speaking, for large inputs an FB filter asymptotically approaches power-law behavior. For example, when the input is an impulse of energy $\mathbf{e}$, the peak of the response v_n asymptotically approaches $k\mathbf{e}^{1/n}$ as $\mathbf{e}$ gets large. When the input is a step of amplitude v_0, the maximum transient response (overshoot) and the steady-state level achieved by the output both approach proportionality to $v_0^{1/(n+1)}$ as v_0 becomes large. Because the output level v_n tends toward the $1/(n+1)$ power of steady inputs, the over-all time constant (which is inversely proportional to the output) also tends towards a power function of the input.

Let $\Delta\mathbf{e}$ be the energy of a small impulse perturbation superimposed on a steady level of input v_0, and let Δv_n and v_n be the amplitudes of the corresponding responses. The sensitivity S of the FB filter, $S=\Delta v_n/\Delta\mathbf{e}$, can be shown to approach a power law, $S\propto v_0^{-n/(n+1)}$. Thus, the amplitude of transient responses and of the steady-state response, the speed of response, and the sensitivity of the FB filter all approach power functions of the input.

Let the Weber fraction W be defined as $W=\Delta\mathbf{e}/v_0$. (The Weber fraction for very brief pulses on a steady background has the units of time.) Writing W in terms of the output pulse gives $W\propto v_n\cdot v_0^{-1/(n+1)}$. For constant W, the response Δv_n increases as $v_0^{1/(n+1)}$. A Weber law (constant W at input gives constant output) never holds for an FB filter; to maintain constant outputs, W must diminish with input. The departure from a Weber law is greater, the smaller the number of FB stages.

The function of the FB filter in the model is to compress the dynamic range of the input. The nervous system does not have sufficient dynamic range to cover the range of possible inputs. For example, the useful range of neuron spike rates is from about 1/sec to 1000/sec, a range of 10^3. The useful range of propagated electrotonic potentials may be somewhat greater but is probably of the same order. When the input is large, a 1-stage FB filter can compress an input range of 10^6 into an output range of 10^3; a 2-stage FB filter can compress an input range of 10^9 into an output range of 10^3. When the input is small, compression is less efficient.

Because the signal that controls the sensitivity of an FB filter is presumed to be a neural signal, it must exert its effect while varying over only a limited range. The FB filter is the only candidate for the function of reducing dynamic range because only the FB filter is controlled by a signal of reduced range (its output). The dynamic range of photopic vision covers about 10^7, ranging from a threshold absorption of probably less than 5 quanta per cone[7] to an upper limit (set by pigment bleaching) of about 10^8 quanta per cone.[8–11] The reduction in range from 10^7 to 10^3 by an FB filter would require it to be of at least two stages. This argument remains valid even if only a few percent of the possible dynamic range are used.

A second function of the FB filter in the model is to reduce the over-all time constant of the system when the input level increases. A similar change of time constant is observed in vision. Presumably it evolved because of intrinsic noise in receptors and in sensory stimuli (e.g., the quantum nature of light). High-intensity signals reach a given signal-to-noise ratio (level of statistical significance) quicker than do low-intensity signals, and a change of time constant of the visual system would reflect a matching to the stimulus.

Delayed Feedforward Filter, FF (Fig. 1c)

We use the notation FF filter for the network shown in Fig. 1(c). The equations representing this network are

$$\frac{d}{d\lambda}v_1(\lambda)+[1+v_0'(\lambda)]v_1(\lambda)=v_0(\lambda) \tag{3a}$$

$$\frac{\tau_D}{\tau_F}\frac{d}{d\lambda}v_0'(\lambda)+v_0'(\lambda)=v_0(\lambda), \tag{3b}$$

with $\lambda=t/\tau_F$. Again, to relate the dimensionless v's of Eqs. (3a) and (3b) to the voltages V of the network in Fig. 1(c), dimensional constants w, μ, and R_0 are required: $v_0(t)=wV_0(t)$, $v_0'(t)=wV_0'(t)$, and $v_1(t)=\mu R_0 w V_1(t)$.

Equation (3a) represents an RC stage with a variable time constant. Here the time constant is given by

$$\tau=\tau_F/[1+v_0'(\lambda)], \tag{3c}$$

where $v_0'(\lambda)$ [given by Eq. (3b)] is the output of a delaying LP stage whose time constant is τ_D and whose input is v_0. For a steady input, the time constant of the FF filter is the same as that of each stage of the FB filter.

Simple (i.e., nondelay) feedforward control in which v_0' is simply equal to v_0 in Eq. (3a) has been proposed for sensory systems by Furman[12] and by Marimont.[13] A simple feedforward system receives identical excitatory and inhibitory inputs, except for magnitude. It is virtually equivalent to a single neuron which receives

[6] The constants in Eqs. (2a–b–c) are chosen to agree with those in Ref. 3.

[7] G. S. Brindley, *Physiology of the Retina and the Visual Pathway* (Edward Arnold Ltd., London, 1960), p. 187f.

[8] Calculated by assuming retinal absorption of 1.4×10^{15} quanta/cm² (Refs. 10, 11) and an average foveal cone density of 1.4×10^7 cones/cm² (Ref. 12).

[9] G. S. Brindley, Proc. Phys. Soc. (London) **68B**, 862 (1955).

[10] W. A. H. Rushton, Ann. N. Y. Acad. Sci. **74**, 291 (1958).

[11] S. Polyak, *The Vertebrate Visual System* (Univ. Chicago Press, Chicago, 1955), p. 268.

[12] G. G. Furman, Kybernetik **2**, 257 (1965).

[13] R. B. Marimont, J. Physiol. (London) **179**, 489 (1965).

identical excitatory and inhibitory inputs, a system which was analyzed by Rall.[14,15]

The delay stage within the FF filter is necessary because at high intensities the signal in the control path is in effect a divisor of the input signal. If the same signal were to act both as input and as control, both as numerator and as denominator, it would in effect cancel itself. The delay acts to spread out the input signal in time, so that the output of the FF filter represents the present input compared to the time-average of recent inputs.

The remarkable characteristic of the FF filter is that in conjunction with any prior linear or power-law component it asymptotically produces a Weber-law system (i.e., one which is sensitive to the ratio of a change relative to a steady baseline rather than to the absolute magnitude of the change). If the input to the FF filter is $W=\Delta v_0/v_0$ (a small pulse superimposed on a steady background) then the output Δv_n is directly proportional to W when v_0 is large. The Weber-law behavior of the model as a whole thus results from the FF filter.

Although a Weber law traditionally has been assumed to imply a logarithmic response characteristic, the FF filter achieves Weber-law sensitivity without having a logarithmic response anywhere in the filter. The FF filter also accentuates the system's sensitivity to differential inputs. In fact, its response to large steady inputs is independent of their magnitude, and only relatively rapid changes of input are reflected in the output.

Threshold Detector

A detector is defined as a stage whose output Y is 1, corresponding to "yes, I see it" (flash, flicker, etc.) or 0, corresponding to "no." In the present case, the output Y is 1 whenever the input varies by more than $\pm\epsilon$; Y is 0 otherwise. We have tried to keep the detector as simple as possible; for example, it has no frequency dependence or statistical uncertainty.

Connecting the Components

The model consists of the components connected in the order shown in Fig. 2, a transducer K to convert units of luminance to units of voltage, the FB filter, followed by the FF filter, the LP filter, and finally the detector. This ordering as well as the function of the various stages in the model is quite well determined. The FB filter must come first in order to reduce the dynamic range; the FF filter converts the model to a Weber-law system; the LP filter sets the temporal-resolution limit; and the detector ultimately makes binary decisions on the last continuous signal. The only uncertainty of the arrangement is whether the LP stages are all lumped together or whether they are interleaved with the other filters. For simplicity, they have been lumped.

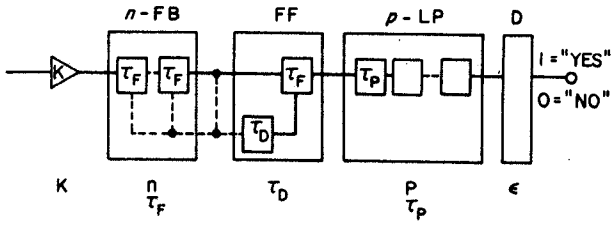

FIG. 2. Block diagram of the model to illustrate signal flow. The parameters to be estimated are indicated under each block: k is a constant to convert luminance units to voltage units; n-FB is a parameter controlled feedback filter of n stages, each with dark time constant τ_F; FF is a parameter controlled delayed feedforward filter also with dark time constant τ_F (the delay stage has time constant τ_D); p-LP is an LP filter consisting of p RC stages each with time constant τ_p; D represents a detector with threshold $\pm\epsilon$.

The results of the next section indicate that n (the number of stages in the FB filter) is two and p (the number of LP stages) is taken as six. This gives a set of ten differential equations which completely defines the model up to the detector. The general solutions of this set of equations are not known to the authors. However, for inputs consisting of steps and pulses, an exact solution has been derived for the FB filter (see Appendix), the solution for the FF stage has been approximated by perturbation analysis, and of course the solution for the linear LP stages is well known. For inputs consisting of sine waves, approximations have been derived for the FB and FF stages by perturbation analysis (see Appendix). The description of the behavior of the model that follows is based primarily on analytic solutions and on small signal approximations; it has also been verified by computer simulation.

II. LUMINANCE DISCRIMINATION

Data

The problem

The classical problem of luminance discrimination may be formulated as follows. Let the system (model or eye) be adapted to an input background luminance until a steady state is reached. Then, let a pulse increment of luminance Δl of duration T be added. What is Δl^*, the minimum detectable Δl, as a function of l and of T? The asterisk is used here to indicate a threshold quantity, or a statistic derived from threshold measurements.

Data statistics

Data from psychophysical luminance-discrimination experiments usually give, for each l, $\log(\Delta l^* \cdot T)$ as a

[14] W. Rall, Exptl. Neurol. 2, 503 (1960).

[15] W. Rall, in R. F. Reiss, *Neural Theory and Modeling* (Stanford Univ. Press, California, 1964), p. 73. The variable-τ RC stage is equivalent to a neuron which receives its excitatory and inhibitory inputs directly onto the soma, which has an equilibrium potential for inhibition (K^+ and/or Cl^- ions) equal to the resting potential, and in which excitation is restricted to small values.

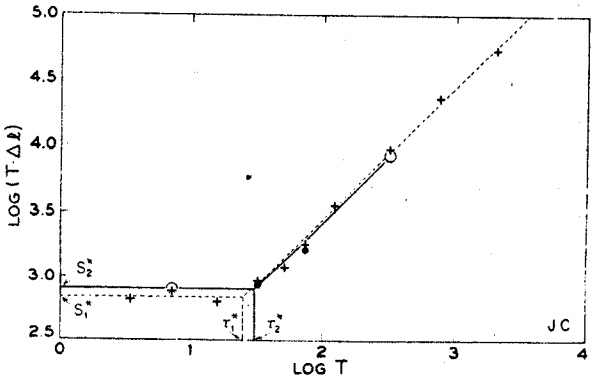

FIG. 3. Log of minimum energy for detection ($-\log S$) as a function of the duration T of a rectangular pulse, illustrating the definition of τ^* and S^*. Data are from Herrick.[18] Background luminance is 470 td; ○●—increment test pulses; +—decrement pulses. Dashed asymptotes were drawn by inspection to data for decrement pulses; their intersections with the axes define τ_1^* and S_1^*. Lines through increment pulses of 7.2 and 314 msec (○) define τ_2^* and S_2^* as described in text. Other increment data (●) are not used in this calculation.

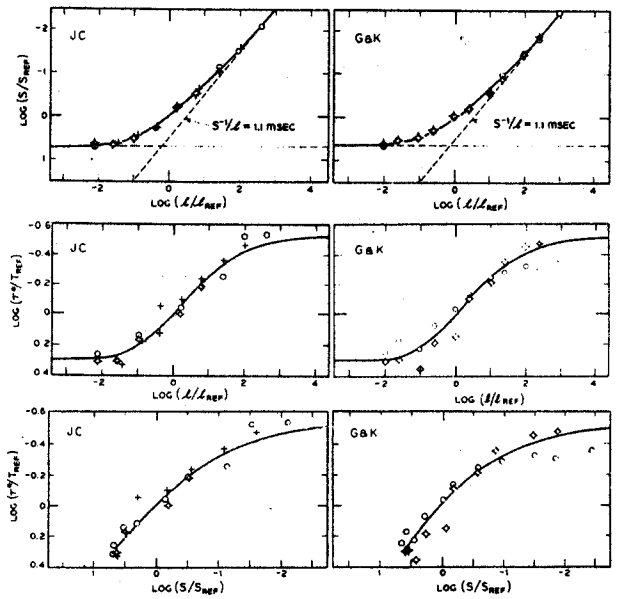

FIG. 4. Comparison of observed values of sensitivity S^* and critical duration τ^* with predictions by the model. Data from Herrick's[18] observer JC (left) and from Graham and Kemp[16] (right). Symbols indicate data on which τ^* and S^* are based. For JC: ○—increment pulses of 7.2 and 314 msec, ◇—increment pulses of 32.1 and 314 msec, +—decrement pulses, asymptotes drawn through all durations. For Graham and Kemp: ●—increment pulses of 5 and 500 msec, ◇—increment pulses of 2 and 500 msec. The lines of slope one in top row of graphs represent asymptotic Weber laws with the indicated Weber constant. Solid curves are generated by the model with shape parameters given in Table I. The coordinates are scaled so that curves pass through (0,0) when $l=l_{ref}$. See Table I for scale factors l_{ref}, τ_{ref}, and S_{ref}.

function of $\log T$. Typical data for just one value of l are illustrated in Fig. 3. At short durations, a horizontal asymptote (representing a constant energy) is drawn through the data; at long durations, a line of slope 1 (representing a constant luminance) is drawn through the data. From these two asymptotes we abstract two significant quantities to characterize the data, sensitivity S^* and critical duration τ^*. The critical duration τ^* is the T-axis value at the point of intersection of the two asymptotes. The sensitivity S^* is the reciprocal of the threshold energy represented by the horizontal asymptote $S^*=\lim_{T\to 0}(\Delta l^* T)^{-1}$. Instead of S^*, we sometimes refer directly to the limiting energy of a short threshold pulse S^{*-1}.

Figure 3 also illustrates graphically a calculation method for computing τ^* and S^* from just two thresholds, one threshold for a long duration T and one for a short duration T. On a log–log plot, a straight line with slope 1 and a straight line with slope 0, respectively, are drawn through the two threshold points. The projections onto the x and y axes of the intersection of the two lines give τ^* and S^*, respectively. The statistics τ^* and S^* thus may be calculated from different threshold pairs in order to illustrate the variability of their estimate. To determine how well the model fits experimental data, rather than examining the undigested data directly, we will examine the relations between predicted and observed values of τ^*, S^*, and l.

Experimental Data

Sufficient experimental data for comparison with the model are available for three observers: Graham and Kemp[16] (one observer) and Herrick.[17] Herrick provided control over pupil size which was lacking in the other study. Herrick's observers viewed a circular field subtending 2°, illuminated to a luminance l, upon which an increment or decrement Δl (also 2°) was superimposed. Figure 4 illustrates the relations between S^* and l, between τ^* and l, and between τ^* and S^* for two observers only, because of space limitations.

The data illustrated in Fig. 4 are based on our analysis of Herrick's original data, which we obtained from the American Documentation Institute.[18] The values of S^* and τ^* for negative (decrement) test flashes were obtained by the asymptote method illustrated in Fig. 3. Values of τ^* for positive (increment) test flashes were obtained by the calculation method, using thresholds measured for pulse lengths of 7.8 and 314 msec and also for pulse lengths of 32.1 and 314 msec (for $\tau^*>40$ msec). Thus, two completely independent values of S^* are available for increment flashes. The two values of τ^* are semi-independent because they share the 314-msec pulse.

Graham's subject viewed a semi-circular field of 38′ radius upon which an increment (same dimensions) was superimposed. An adjacent comparison field did not receive the increment but because of an 8′ boundary

[16] C. H. Graham and E. H. Kemp, J. Gen. Physiol. 21, 635 (1938).

[17] R. M. Herrick, J. Comp. Physiol. Psychol. 49, 437 (1956).

[18] ADI Document No. 4989 ($1.25), Library of Congress, Washington, D. C. 20540.

dividing the two fields, we doubt that the comparison field influenced the results.

Our analyses of Herrick's[18] and of Graham and Kemp's[16] data generally agree with their analyses except for one important difference. Both authors conclude that the relation between log$l$ and logτ^* is linear. While this approximation may be valid for a middle range of luminances, τ^* appears to reach limiting values both at very low and at very high luminances. Our calculations also reveal a small but consistent difference of τ^* between increment and decrement test flashes for Herrick's observer JB.

Predictions by the Model

To specify the model completely we need to estimate the values of seven constants: n, τ_F, τ_D, p, τ_p, ϵ, and k. Here, n is the number of stages in the FB filter, τ_F is the dark time constant of the variable stages in the FB and FF filters, τ_D is the time constant of the delay stage in the FF filter, p is the number of LP stages, τ_p is their time constant, ϵ is the threshold of the detector, and k is a factor relating input luminance to the voltage units of the model. This array of constants is less formidable than it appears.

To begin with, overwhelming experimental evidence[19,20] indicates that $n+p$ is large, e.g., ≥ 8. Since n is 2 (see below), $p>5$. For five or more cascaded stages, the impulse response of an LP filter is approximately gaussian with only one significant parameter—the over-all time constant. This means that p and τ_p represent only one independent parameter. Hence we arbitrarily fix $p=6$ and vary τ_p to obtain the desired over-all time constant for the LP filter.

The functional requirement for the FB filter (for dynamic-range reduction) had indicated $n=2$ (Sec. I). Anatomical considerations (Sec. IV) suggest $n=1$ although $n=2$ cannot be excluded. Comparison of the model with data clearly excludes values of $n\geq 3$, and excludes $n=1$ for two of the three subjects. The constant n thus is fixed at 2 and should be regarded as a stable feature of the model rather than as a parameter.

Estimation of Parameters

The five constants which remain may vary from subject to subject and therefore are parameters of the model. Of these five parameters, three are scale factors (i.e., they relate units of measurement) and two alter the behavior of the model.

When the ratios τ_D/τ_F and τ_p/τ_F are kept fixed then, except for scaling (choice of origin in log–log graphs), the behavior of the model is independent of the choice of values for the parameters τ_F, k, and ϵ. Here we assume that, at any background luminance, the eye—like the model—is approximately linear for inputs near threshold. Our estimation procedure utilizes the small-signal linearity of the model.

TABLE I. Estimated shape parameters and scale factors of the model: τ_F as determined from scale factor for time axis also is indicated. Values for τ are in msec, for l in trolands, and for $1/S$ in msec×trolands. (For Graham and Kemp,[16] l is in mL and $1/S$ is in msec×mL.)

Observer	τ_p/τ_F	τ_D/τ_F	l_{ref}	τ_{ref}	$1/S_{ref}$
Herrick,[18] JC (DeLange,[19] L)	4.7/29.0	11.5/29.0	17.6(10)	55	56.5
Herrick, JB	8.5/19.0	10.0/19.0	125	44	236
Graham & Kemp[16]	4.2/25.0	20.0/25.0	0.20	56	0.74
DeLange, V	5.7/25.0[a]	15.0/25.0[a]	10	50	

[a] Nominal value, insufficient data for estimation.

Another property that simplifies estimation is that at low luminances the effect of the six LP stages is almost negligible compared to that of the three controlled stages (2-FB plus 1-FF) and at high luminances the reverse is true. When the number of stages of time constant τ is three and six, respectively, the factors 3.7 and 5.7 express the factors by which τ must be multiplied to give critical duration τ^*. Thus, the dark critical duration of the model is approximately 3.7 τ_F (owing to the three cascaded RC filters each with a time constant of τ_F) and the critical duration at a very high luminance approaches 5.7 τ_p (owing to the six stages of the LP filter).

To estimate parameters, we start with the ratio of the subject's critical duration in the dark to his critical duration in extremely high luminances. The ratio of these two critical durations estimates $5.7\,\tau_p/3\cdot 7\tau_F$. We chose the ratio τ_D/τ_F arbitrarily (a good starting value is about $\frac{1}{2}$). These two parameters completely determine the shapes of the logS^* vs l, logτ^* vs log$l$, and logτ^* vs logS^* curves predicted by the model.

The translations on a log–log graph which are required to bring the predicted curves into coincidence with a subject's performance determine the parameters k, ϵ, and the time-scale factor. Suppose l^*_{ref} is the adaptation luminance at which the subject's critical duration is exactly half of its value in the dark. Let S^*_{ref} and τ^*_{ref} be his sensitivity and critical duration at $l=l_{ref}$. Identifying l_{ref} with the input voltage required by the model to halve its critical duration determines k. The perturbation at the input to the model corresponding to the subject's impulse threshold S^{*-1} at $l=l^*_{ref}$ determines ϵ. The subject's value of τ^*_{ref} determines the time unit of the model. The parameters obtained in this way are only approximate because the trial value of τ_D might not be accurate and also because the critical durations in the dark and at very high luminance depend somewhat on all of the time constants. Therefore, the parameters are iteratively perturbed until a best fit to the data results. The parameter values are shown in Table I; the predictions of the data generated by these parameters are shown in Fig. 4.

[19] H. DeLange, J. Opt. Soc. Am. 48, 777 (1958).
[20] D. H. Kelly, J. Opt. Soc. Am. 51, 422 (1961).

In order to limit the number of estimated parameters, several factors were assigned values *a priori* even though their values normally would be estimated *a posteriori*. For example, the time constants of each of the stages of the FB filter and also of the variable stage of the FF filter were arbitrarily taken to be the same. The inputs to the delay stage and to the through stage of the FF filter were taken to be equal in magnitude. The feedback signal in the FB filter was assumed to act with zero delay, clearly an oversimplification. Although these assumptions are not correct, the error—if it is not too large—may be compensated by variations of the values of the estimated parameters. For this reason, the time constants in Table I should not be taken too literally as estimates of underlying processes.

Goodness of Fit

Inspection of Fig. 4 shows the fit of theory to data is quite good. For example, the model's prediction of $\log S^{*-1}$ vs $\log l$ agrees with the observed data within measurement error, including the asymptotic Weber laws for high luminance (lines of slope=1). The goodness of predictions of τ^* is more difficult to evaluate because of the greater variability of the data (estimates of τ^* require measurement of thresholds with at least two different conditions) and because of the small range of variation of τ^* (e.g., in Fig. 4 the scale for τ^* is expanded by 3.5 over the scale for S^*).

The Number of Stages with Variable τ

For a pure n-stage FB filter, $\partial \log S^*/\partial \log \tau^* = n$. For such a system, the $\log \tau^*$ vs $\log S^*$ curves at the bottom of Fig. 4 would be straight lines of slope $1/n$. Fuortes and Hodgkin[3] used this property of FB filters to estimate the number of variable stages in *Limulus* as 7 to 14. If a system is not pure FB, particularly if it contains some fixed-τ stages (e.g., LP stages), then $\partial \log S^*/\partial \log \tau^*$ may fail to estimate the number of variable-τ stages. For example, the slopes of the $\log \tau^*$ vs $\log S^*$ functions in Fig. 4 vary from $\frac{1}{2}$ to 1/50. In a pure FB filter these slope values would indicate 2 to 50 variable-τ stages; in Fig. 4 they result from exactly three variable-τ stages (2-FB, 1-FF) in conjunction with an LP-filter observed at different adapting luminances. Similarly, Levinson's[21] argument (from the slope of $\log \tau$ vs $\log l$) that there are 6 variable-τ stages would be valid only if the entire system were a pure FB filter, not otherwise.

III. FLICKER DETECTION

The Problem

The most general and best studied case of flicker detection is the detection of a sinusoidal modulation m superimposed on a steady luminance l.[22,23] Sinusoidal-flicker experiments seek to determine the threshold amplitude of sinusoidal modulation as a function of frequency (the function is called a DeLange characteristic) at various levels of background luminance. From the results with sine-wave modulation (DeLange characteristics), it is possible to predict the results of all other flicker experiments which use periodic stimuli (e.g., square waves, impulses, etc.) at repetition rates greater than about 5–10 Hz.[24] DeLange characteristics thus predict the bulk of the available flicker detection data. Without loss of generality we therefore limit our predictions of flicker to DeLange characteristics.

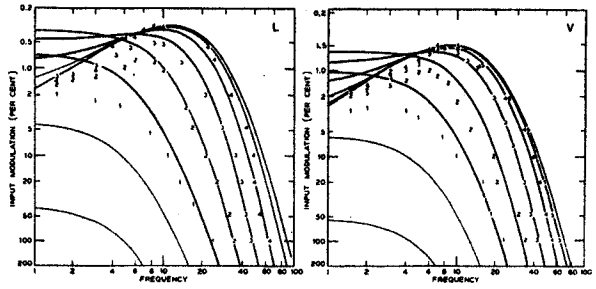

FIG. 5. Comparison of observed with predicted sinusoidal-flicker thresholds. The theoretical DeLange characteristics are predicted by model with parameters given in Table I. Data are from DeLange's[19] observers L (left) and V (right). Luminance in trolands is indicated by the plotted symbols: "1"=1, "2"=10, "3"=100, "4"=1000, "5"=10 000 (observer V only). Some data at intermediate luminance values have been omitted for clarity. The lightly drawn theoretical curves indicate predictions for two higher (one higher, observer V) and for two lower luminance values than were studied. The curve for highest luminance is virtually identical to the envelope of the series of curves.

Data and Theory

Figure 5 illustrates data from DeLange's[19] observers L and V. The set of theoretical DeLange characteristics illustrated for observer L were predicted by the model, using the same time constants as for Herrick's observer JC. The predicted curves for observer V are based on new estimated parameters (see Table I).

DeLange's viewing conditions were similar to Herrick's (2° circular field, foveal fixation) except that DeLange surrounded his test field with a steady uniform background (60° diam, luminance l). In principle, the model with the parameters estimated for Herrick's pulse-discrimination data could be applied directly to DeLange's flicker data, but two adjustments are necessary. First, the vertical position of the set of theoretical curves has been adjusted to give an approximate best fit. This adjustment corresponds to diminishing ϵ, the detection threshold, by a factor of about ten.[25] Second,

[21] J. Levinson, J. Opt. Soc. Am. **56**, 1442A (1966).
[22] H. E. Henkes and L. H. van der Tweel, Eds., *Flicker* (Dr. W. Junk, Publishers, The Hague, 1964).
[23] J. L. Brown, in G. H. Graham *et al.*, *Vision and Visual Perception* (John Wiley & Sons, Inc., New York, 1965), p. 251.
[24] D. H. Kelly, Doc. Ophthalmol. **18**, 17 (1964).
[25] Unpublished data of J. Levinson in which flicker and pulse thresholds are compared directly in the same observer under the same conditions, indicate that the model's ϵ-discrepancy (between flicker and pulse thresholds) is a factor of 2. Much of the discrepancy vanishes if predictions are made from peak-to-peak instead of from average-to-peak (personal communication).

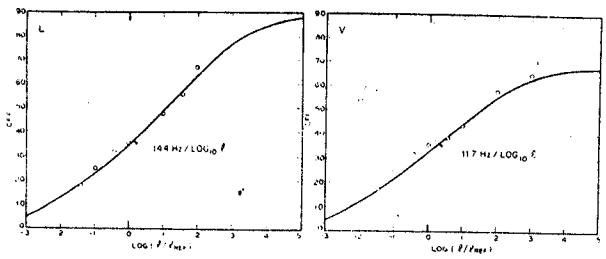

FIG. 6. Critical flicker frequency (CFF for 100% sinusoidal modulation) as a function of luminance. The data are from DeLange[19] and include intermediate values omitted from Fig. 5. The theoretical predictions are the same as in Fig. 5. The slope of the approximately straight line segment of the curves is indicated in Hz/$\log_{10}l$ (Ferry–Porter constant).

a slightly better fit (for observer L) was obtained after dividing the luminances stated by Herrick by 1.8 (i.e., changing k) instead of using them directly. The discrepancy between an artificial-pupil system (Herrick) and a maxwellian-view system (DeLange) might well be as large as 2, and we preferred this adjustment to changing the time constants of the model.

The theoretical predictions fit the experimental data well for frequencies above about 8 to 10 Hz. The critical flicker frequency CFF (obtained at 100% sinusoidal modulation) is illustrated in Fig. 6. The prediction of CFF is within measurement error.

Although the function relating CFF to log Hz is S shaped, it may have a nearly linear middle portion (Ferry–Porter law) which extends for several log units of luminance.[23] The model predicts Ferry–Porter laws with slopes of about 14.6 and 11.7 Hz/$\log_{10}l$, for observers L and V, which are good fits in this instance.

The good fit of the model—with time constants estimated for observer JC—to observer L is fortuitous. A fit to DeLange's observer V requires slightly different parameters than those estimated for the three observers whose luminance discrimination we have been able to study.

At frequencies below 10 Hz, the model increasingly overestimates an observer's ability to detect flicker. This overestimation is inherent in the model for all reasonable values of the parameters and is considered in Sec. V.

IV. SOME RELATIONS OF THE MECHANISM OF THE MODEL TO THE MECHANISMS OF VISION

Neural Identification of the Model's Components

RC Stage

In comparing components of the model with neural structures, the critical analogy is between an RC stage and those portions of a neuron which are concerned with synaptic transmission. That the resistance and capacitance of a neuron—in conjunction with its geometry—can be related directly to the R and C of an equivalent RC stage is now abundantly documented.[1,2,14,15,26,27] Signals received by a neuron through excitatory synapses produce a neural voltage which is represented as a voltage input to the equivalent RC stage; signals received by a neuron through inhibitory synapses produce a resistance change in the neural membrane which is equivalent to a resistance change in the equivalent RC stage.

In addition to their main effect, excitatory neural signals produce a secondary resistance change (which becomes significant for large signals) and inhibitory signals usually produce a secondary effect equivalent to a voltage input. These secondary effects have been neglected in our simplified RC analogy, which also implicitly assumes that synapses are positioned on the neuron soma. Synapses on dendrites produce comparable neural signals except that the path from the dendrite to soma must be considered[15]; it may be approximately represented by one or more LP stages.

Little systematic information about retinal synaptic connectivity was available at the time the model was formulated, so it was based on functional considerations. But, except for the detector, the functional model is composed of RC components, each of which has a neural analogy. Insofar as we accept the RC stage—neuron analogy, a functional model implies a neural model and *vice versa*. We now compare, component by component, the model implied by our functional analysis with retinal models implied by microanatomical and physiological research.

The macrostructure of the retina is quite clear: **cones** and **rods** (the receptors) connect via various kinds of **bipolar** cells to **ganglion** cells whose axons form the optic nerve. Various kinds of **horizontal** cells lie near the receptor–bipolar interface while various kinds of **amacrine** cells lie near the bipolar–ganglion interface.[11]

FB Filter

The function of the FB filter is to compress the dynamic range of luminance inputs. In the eye, physiological evidence places the compression of dynamic range at and near the receptor level.[28]

The synaptic connections at the receptor level still are not well known. However, it has been shown that cones have a double synapse to horizontal cells and to midget bipolars, a single synapse to flat bipolars, and that a single horizontal cell connects to numerous cones.[29,30] From these anatomical observations, Dowling and Boycott[31] infer that horizontal cells carry a feedback signal to the cones. The microanatomy suggests

[26] J. C. Eccles, *The Physiology of Synapses* (Springer-Verlag, Berlin, Göttingen, Heidelberg, 1964).
[27] For a review see B. Katz, *Nerve, Muscle, and Synapse* (McGraw-Hill Book Co., New York, 1966).
[28] K. T. Brown and K. Watanabe, Science 148, 1113 (1965).
[29] J. E. Dowling, Science 147, 57 (1965).
[30] L. Missoten, *The Ultrastructure of the Retina* (Arscia, Brussels, 1965).
[31] J. E. Dowling and B. B. Boycott, Proc. Royal Soc. (London) 166B, 80 (1966/67).

a modified 1-stage FB filter, in which the RC stage (cone synapse onto bipolar) is controlled by delayed feedback (through the horizontal cell). Our functional FB filter consists of two stages with no delay of feedback. However, the simplifying assumptions of our RC analogy are most vulnerable at the receptor level (because of the high levels of input), and the synaptic connectivity still is uncertain (for example, there are numerous other possible paths for inhibition[30,32–35]), so it is premature to press the comparison further.

FF Filter

We propose the FF filter as the mechanism by which the ganglion cell's receptive field is organized, with the controlled signal originating from the center of the receptive field and the controlling signal from the surround. In this theory, the FF filter is a representation of the neural interactions occurring at the level of the bipolar–ganglion cell interface. The delayed controlling signal passes through the amacrine cells. The large spatial extent of these cells corresponds to the surround area of the receptive field.

Bipolars transmit to ganglion cells through a double synapse, the second half of which transmits to amacrine cells.[36] The amacrine then retransmits to the bipolar via a simple synapse in the immediate neighborhood, thereby providing a local inhibitory path (bipolar–amacrine–bipolar) which is feedback (the amacrine receives the bipolar's output signal and feeds it back to the bipolar). As a bipolar axon meanders through the inner plexiform layer, it makes numerous such connections.[31] Such a series of recurrent loops (bipolar–amacrine–bipolar) forms a complex attenuating channel whose analysis is beyond the scope of this article.[37]

Signals from the center of the ganglion cell's receptive field travel via the bipolar attenuating channel and connect only onto the ganglion cell's dendrites (except in the case of rod bipolars which make some additional connections to the soma of diffuse ganglion cells).[31] Signals from the surround portion of the ganglion cell's receptive field travel via amacrine cells and generally connect to both dendrites and soma of ganglion cells. The separation between the two avenues of input to the ganglion cell serves to increase the effectiveness of the surround's control over the center.[38] Because ganglion cells themselves do not transmit back to the retina, they provide no feedback paths. Therefore, in ganglion receptive fields, control of the center by the surround must be feedforward.

LP Filter

For a small dynamic range of inputs, a variable-time-constant RC stage can be approximated by a fixed-time-constant LP stage. The two FB stages and the FF filter greatly reduce the dynamic range of input signals; the model is applied mainly to predicting barely detectable signal modulations; therefore, we approximate the contribution to detection of subsequent neural interactions by LP stages.

The six (or more) LP stages limit the high-frequency response. Their average time constant of approximately 5 msec is typical for excitatory post-synaptic potentials in fast neurons.[39] However, the number of LP stages and the time constant of each is not critical for the model—only the over-all time constant is critical.

Although the LP stages of the model were lumped together for convenience, it probably would have been more accurate to place some LP stages between (and within) the FB and FF filters. LP stages represent the low-pass filtering which occurs when signals travel long dendritic paths[15] and such paths occur in the neurons which the FB and FF filters are presumed to represent. The remaining LP stages of the model represent synapses beyond the retina. These LP stages cause appreciable differences of attenuation only at high input frequencies ($\approx$3 dB per octave above 30 Hz for each LP stage of $\tau_p = 5$ msec). For visual inputs that flicker at high frequencies, the ERG[40] and some centrally recorded evoked responses[41] to flicker are much greater than would be expected from psychophysical CFF data. The model predicts that this would occur whenever some synapses (LP stages) still remain to be traversed between the site of recording and the site of detection.

Impulse Response and Analogy to Spatial Vision

Figure 7 illustrates the impulse response of the model, just prior to the detector. The input consists of a small impulse $\Delta l \cdot \delta(t)$ superimposed on a steady background of luminance l. Outputs are illustrated for ten values of l, each background differing from the previous one by 10×. The range is from infinitesimal l (the first three impulse-response curves superimpose exactly) to an intense l (correspondingly roughly to 0.7×10^6 td). The response curves have been normalized so their maxima equal 1. The shape parameters are those illustrated for Herrick's observer JC; other sets of

[32] M. Kidd, J. Anat. (London) **96**, 179 (1962).
[33] W. K. Stell, Anat. Record **153**, 389 (1965).
[34] J. E. Dowling, J. E. Brown, and Diane Major, Science **153**, 1639 (1966).
[35] A. I. Cohen, J. Anat. (London) **99**, 595 (1965).
[36] J. E. Dowling and B. B. Boycott, Cold Spring Harbor Symp. Quant. Biol. **30**, 393 (1966).
[37] If the internal resistance of the bipolar axon is small, then the sequence of recurrent loops it generates as it connects to various ganglion-cell dendrites can be represented by a single 1-stage FB filter. The anatomy then provides two successive 1-stage FB filters, each with delayed feedback, a system which is similar to the 2-stage FB filter of the model.
[38] For a similar separation of the loci of excitation and of inhibition in a peripheral visual neuron, see R. L. Purple and F. A. Dodge, Cold Spring Harbor Symp. Quant. Biol. **30**, 529 (1966).
[39] D. R. Curtis and J. C. Eccles, J. Physiol. (London) **145**, 529 (1959).
[40] L. H. van der Tweel, Doc. Ophthalmol. **18**, 287 (1964).
[41] A. S. Schwartz and D. B. Lindsley, Bol. Inst. Estud. Med. Biol. (Mex) **22**, 249 (1964).

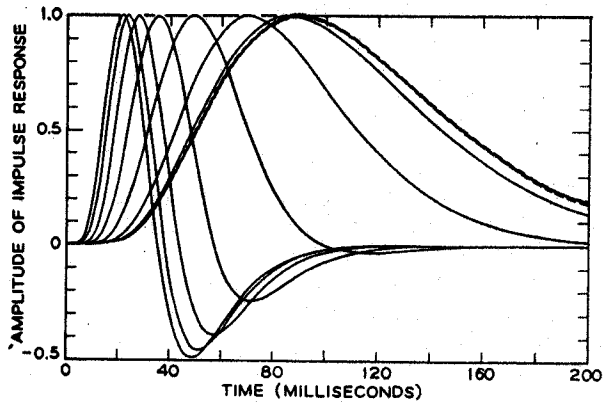

FIG. 7. Response of model to small impulses $[\Delta I \cdot \delta(t)]$ superimposed on backgrounds ranging in luminance from 0.7×10^{-3} td to 0.7×10^{6} td. Successive background luminances differ by 10 X. The responses have been scaled to have the same maximum height; responses at the three least luminous backgrounds are superimposed.

parameters from Table I produce highly similar families of curves.

Similarity between Temporal and Spatial Receptive Fields

Physiologists call an inverse relation between an input and an output (neuron-spike frequency) inhibition. A direct relation is called excitation. These terms also apply to phases of a response. The impulse response curves of Fig. 7 illustrate nicely the change from pure excitation at low luminances to excitation plus inhibition at moderate and high luminances. The first indication of inhibition—a significant undershoot in the impulse response curve—occurs with background luminances greater than about 10^2 td. At adapting luminances of about 10^4 td and greater, the negative portion of the impulse response balances the positive portion almost exactly so that the integral over the whole impulse response is virtually zero; thus, net inhibition equals net excitation.

Let impulses be superimposed on a series of backgrounds of diminishing luminance. The change of the impulse response with this controlled dark adaptation is from excitation plus inhibition at high background levels to excitation only for backgrounds below 10^2 td. If the model were stimulated only at a single instant (impulse input), and the response recorded only at a single instant, then by varying the time of stimulation, an excitatory region (of times) and an inhibitory region (of times) would be observed; i.e., the impulse response could be laboriously reconstructed. The temporal inhibitory period would be observed to be spread out relative to the excitatory period, and it would be observed to disappear with dark adaptation (Fig. 7).

The properties of the temporal receptive field (of the model) are close analogs of the properties of spatial receptive fields observed in retinas[42] and deduced from psychophysical experiments.[43–45] Insofar as there is a single mechanism for the organization of the receptive field, parallelism between temporal and spatial phenomena is inevitable. Barlow *et al.*,[42] attributed the changes of spatial mode of response to "change of organization in the receptive fields of the cat's retina," (with the implication of a change of connectivity). In the model, these properties result from a single kind of connectivity which causes vastly different responses to the same input signal depending on whether it is superimposed on high or on low levels of background illumination.

V. DISCUSSION

Errors of Prediction

As a point of reference, consider the model with its detection parameter ϵ chosen appropriately for flicker detection at frequencies above 10 Hz. Then it predicts single-pulse thresholds and low-frequency sine-wave modulation thresholds which are lower than those actually observed. The flicker experiments[19] used a background field equal in luminance to the test, and the pulse-detection experiments[16,18] did not. This difference of viewing conditions produces systematic threshold shifts and therefore leads to prediction errors by the model because the model does not deal explicitly with spatial parameters.[25] Below, we consider three other factors which lead to prediction errors.

Sampling Effects

Due to quantum fluctuations of the stimulus[46,47] and to internal noise in the visual system,[48] the actual input to the detector will fluctuate around the predicted mean value. The same physical stimulus presentation may thus exceed threshold on some trials and fail to exceed threshold on other seemingly identical trials. This trial-to-trial variability is well known and an elaborate technology has been developed to deal with it.[49,50] In a pulse-detection experiment, such as Herrick's,[17] trials are well separated. On each trial, the pulse is either present or absent. The observer is constrained to set his criterion (the value of ϵ in the model) at a sufficiently large value so that on trials when no signal is presented, he gives an acceptably low level of false positive detections (e.g., <0.05). The stimulus threshold is defined as the value of $\Delta I \cdot T$

[42] H. B. Barlow, R. Fitzhugh, and S. W. Kuffler, J. Physiol (London) **137**, 327 (1957).
[43] R. Ratoosh and C. H. Graham, J. Exptl. Psychol. **42**, 367 (1951).
[44] W. M. Kincaid, H. R. Blackwell, and A. B. Kristofferson, J. Opt. Soc. Am. **50**, 143 (1960).
[45] G. Westheimer, J. Physiol. (London) **190**, 139 (1967).
[46] A. Rose, J. Opt. Soc. Am. **38**, 196 (1948).
[47] H. DeVries, Physica **10**, 553 (1943).
[48] H. B. Barlow, J. Physiol. (London) **136**, 469 (1957).
[49] H. R. Blackwell, J. Opt. Soc. Am. **53**, 129 (1963).
[50] J. A. Swets, *Signal Detection and Recognition by Human Observers* (J. Wiley & Sons, Inc., New York, 1964).

which is detected on 0.5 of the trials on which it is presented.

We consider now a flicker experiment in which brief pulses are presented at a rate of 10/sec. If the observer maintained his pulse criterion in the flicker experiment, it would imply that 50% of the pulses (i.e., about 5 pulses/sec) exceeded the detection criterion. In the usual flicker experiment, the observation period is several seconds, often tens of seconds. Under such conditions, a criterion which required 0.5 of the pulses to exceed threshold is excessively stringent. Good discrimination between flickering and steady luminances theoretically is possible even if only 5% or 10% of the pulses (i.e., one pulse every few seconds) exceeds threshold. Lacking quantitative data about the amplitude and the frequency spectrum of noise fluctuations of the input to the detector, we cannot predict the criterion factor relating flicker thresholds to pulse thresholds.[51] An order-of-magnitude calculation of the effect of a criterion difference between the flicker and single-pulse thresholds suggests that it may account for a factor of about three between flicker and single-pulse predictions.

Perfect Memory in the Detector

Another factor which is particularly important in the low-frequency predictions of the model is the assumption that the detector's memory of its input is perfect, so that whenever a perturbation by as much as ϵ occurs, it is detected. Absolute memory for luminance is remarkably poor,[52] even though much luminance information demonstrably is available at the time of stimulation.[53] The incorporation of a limited memory capacity in the detector would improve the prediction of low-frequency sine-wave modulation thresholds. The unique difficulties of predicting low-frequency modulation thresholds also have been recognized by other theorists[54]; most of these difficulties seem to be attributable to the great role of nonretinal factors in determining these thresholds.

Contrast Detection (Simultaneous Luminance Discrimination)

Let an increment of luminance Δl be added to only a portion of a uniform field of luminance l. An observer may be able to detect Δl by spatial comparison of l with $l+\Delta l$ even when he has failed to detect the temporal change. The use of spatial information to detect Δl is called contrast detection. Contrast detection appears to involve a slightly different mechanism than temporal luminance discrimination (successive luminance discrimination), and the present model applies only to experiments in which contrast detection is excluded.

In DeLange's flicker experiments,[19] a background field was available for contrast detection. By providing an external reference, the background functions in much the same way as would improved memory for luminance. The presence of a background tends to reduce the prediction error at low frequencies of flicker, so that the model's true prediction error is greater than that illustrated in Fig. 5.

In Graham and Kemp's experiment,[17] an adjacent comparison field, which did not receive the increment of luminance, was available for potential use in contrast detection. Because of a separation between the incremented and the unincremented areas, the presence of the comparison field seems not to have influenced the data. This illustrates that available contrast information need not necessarily be utilized.

In an experiment intended to elaborate Graham and Kemp's findings, Biersdorf[55] superimposed an increment on a larger field. He also instructed his subjects to report not when they merely discriminated the presence of the increment, but only when they saw it as a disk. Biersdorf's procedure probably involves contrast detection, particularly at high background illumination, and invalidates comparison with the studies considered here. It also may account for Biersdorf's quite different results. Other well known studies that appear to be relevant to the present model but must be excluded because they involve contrast detection are those of Kahneman.[56,57]

VI. SUMMARY AND CONCLUSIONS

The model proposed here consists of three types of filters in cascade, plus a detector. The universal element in all filters is an RC stage whose time constant τ is a variable, signal-controlled parameter. The variable-τ RC stage is a good approximation to a neural excitatory process controlled by synaptic inhibition.

The first filter (parametric feedback filter FB) consists of two RC stages in cascade. Its input is a retinal illumination which varies as a function of time; its output controls the time constants of both its RC stages (parametric feedback control). The FB filter represents retinal interactions at the receptor–bipolar level, with the controlling signal passing through the horizontal cells.

The second component is a parametric feedforward

[51] For various different assumptions that have been made about noise distribution to enable theoretical estimates of the effects of visual noise on flicker thresholds see R. C. Jones, Washington Acad. Sci. 47, 100 (1957); L. H. van der Tweel, Ann. N. Y. Acad. Sci. 89, 829 (1961); and D. H. Kelly, J. Opt. Soc. Am. 51, 747 (1961).

[52] G. H. Mowbray and J. W. Gebhard, in W. H. Sinaiko, Ed., *Selected Papers on Human Factors in the Design and Use of Control Systems* (Dover Publications, Inc., New York, 1961).

[53] T. N. Cornsweet and H. M. Pinsker, J. Physiol. (London) 176, 294 (1965).

[54] See, for example, J. Levinson and L. D. Harmon, Kybernetik 1, 107 (1961).

[55] W. R. Biersdorf, J. Opt. Soc. Am. 45, 920 (1955).

[56] D. Kahneman and J. Norman, J. Exptl. Psychol. 68, 215 (1964).

[57] D. Kahneman, J. Exptl. Psychol. 71, 543 (1966).

filter FF. It consists of an RC stage whose time constant is controlled indirectly by its input signal (parametric feedforward control). The controlling signal itself passes through an RC stage (delay stage) before affecting the time constant. The FF filter represents retinal interactions at the bipolar–ganglion cell level, with the controlling signal passing through the amacrine cells.

The third component consists of six (or more) RC stages in series, each with the same, fixed, time constant. These represent dendritic delays within the retina and synapses beyond the retina.

Finally, the detector detects a signal whenever its input (the output of the sixth RC stage) varies from a steady level by more than $\pm\epsilon$. The detector is nonretinal and tentatively of minimum complexity.

The equations generated by the model were solved and applied to predicting the results of luminance discrimination experiments, (i.e., an observer detects a luminance increment or decrement which is of variable duration and superimposed on a background of variable luminance). By estimating two time constants (and three scale factors) for each subject, very good fits to individual data were obtained, including estimates of the dark- and the light-adapted critical duration, the dark-adpated sensitivity, and the constant of the asymptotic light-adapted Weber law.

In sinusoidal-flicker experiments, a subject detects the flicker of a sinusoidally modulated light as a function of the modulation depth, the modulation frequency, and the luminance of the light being modulated. The model, with the same time constants as were estimated for luminance-discrimination experiments, gave good predictions of flicker thresholds for frequencies above 10 Hz, including accurate predictions of the Ferry–Porter law relating CFF (for 100% modulation) to luminance.

Errors of the prediction of low-frequency flicker thresholds and a decrease of the detection criterion from pulse-detection to flicker-detection predictions were attributed to the following factors: differences of psychophysical procedure, the implicit assumption of perfect memory for the detector, and the neglect (in the model) of internal and external sources of noise.

It is concluded that the model of visual interactions, which is consistent with available physiological and anatomical data, can predict the results of luminance discrimination and of flicker detection experiments with considerable detail, accuracy, and economy.

APPENDIX

This appendix outlines the methods used for solving the sets of Eqs. (2) and (3). We use the notation $D=d/d\lambda$.

In the Eqs. (2) the substitution

$$F(\lambda)=\exp\left(\int_0^\lambda [1+v_n(\lambda')]d\lambda'\right) \tag{A1}$$

is equivalent to the substitution

$$DF(\lambda)=F(\lambda)[1+v_n(\lambda)] \tag{A2}$$

and gives

$$D[F(\lambda)v_j(\lambda)]=F(\lambda)v_{j-1}(\lambda) \quad j=1,\cdots n. \tag{A3}$$

From Eqs. (A3), by substituting the j-th equation in the $(j+1)$-th with j going from 1 to $n-1$, we get

$$D^n[F(\lambda)v_n(\lambda)]=F(\lambda)v_0(\lambda). \tag{A4}$$

Hence, from Eq. (A2)

$$D^{n+1}F(\lambda)-D^nF(\lambda)-v_0(\lambda)F(\lambda)=0. \tag{A5}$$

Thus the set of first-order nonlinear Eqs. (2) is transformed to a single linear Eq. (A5) of order $n+1$ in the variable F. The solution of Eq. (A5) gives the complete solution of the set (2). For given $F(\lambda)$, $v_n(\lambda)$ is obtained from Eq. (A2) and, if desired, $v_1(\lambda)\cdots v_{n-1}(\lambda)$ from the Eqs. (A3). Note also that the solution of Eq. (A5) readily provides the solution for the case when an $(n+1)$-th simple, nondelayed feedforward stage is cascaded. This is because the equation for such a stage is

$$D[F(\lambda)v_{n+1}(\lambda)]=F(\lambda)v_n(\lambda) \tag{A6}$$

or, from Eq. (A2),

$$v_{n+1}(\lambda)=\frac{1}{F(\lambda)}\left[\int_0^\lambda [DF(\lambda')-F(\lambda')]d\lambda'-F(0)v_{n+1}(0)\right]. \tag{A7}$$

Step and Pulse Inputs

For arbitrary $v_0(\lambda)$ we do not have a method for the exact solution of Eq. (A5). However, for $v_0(\lambda)$ consisting of combinations of step functions and impulses the exact solution can be obtained. We will illustrate this by one example.

Consider an input $v_0(\lambda)=Au(\lambda)+B\delta(\lambda-\lambda_0)$ applied to the system which is initially quiescent $[v_0(\lambda)\equiv 0, \lambda\leq 0]$. The input is a step change in illumination at $\lambda=0$ on which is superimposed a flash at $\lambda=\lambda_0$. Then Eq. (A5) becomes

$$\begin{aligned}(D^{n+1}-D^n-A)F(\lambda)&=0, \quad \lambda<\lambda_0\\ &=BF(\lambda_0)\delta(\lambda-\lambda_0), \quad \lambda\geq\lambda_0.\end{aligned} \tag{A8}$$

The solution of Eq. (A8) may be obtained by standard methods, using the fact that at $\lambda=0$, $F(\lambda)$ and all its derivatives are equal to 1. The solution of Eq. (A8) is

$$\begin{aligned}F(\lambda)&=\sum_{i=0}^n a_i\exp(s_i\lambda), \quad \lambda\leq\lambda_0\\ &=\sum_{i=0}^n a_i\exp(s_i\lambda)+\frac{B}{A}\left(\sum_{i=0}^n a_i\exp(s_i\lambda_0)\right)\\ &\quad\times\sum_{i=0}^n a_i(s_i-1)\exp[s_i(\lambda-\lambda_0)], \quad \lambda\geq\lambda_0.\end{aligned} \tag{A9}$$

Here s_i are the roots of

$$S^{n+1}-S^n-A=0, \tag{A10}$$

and

$$a_i=s_i/[(n+1)s_i-n]. \tag{A11}$$

Using Eq. (A2), we see that the solution for $v_n(\lambda)$ is expressed as a ratio of the sums of exponentials and damped sine and cosine terms.

The method outlined above is adequate, with appropriate minor modifications, for other combinations of pulses and steps and for different initial conditions (e.g., the system could be adapted to a steady input other than zero). The solution of the characteristic Eq. (A10) is cumbersome for $n>2$. However a variety of efficient subroutines for solution of polynomial equations by computers are available.

Sinusoidal Inputs

We consider the solution of Eq. (A5) when

$$v_0(\lambda)=A(1+m\cos\omega\lambda). \tag{A12}$$

A perturbation solution is obtained by the following method.

We consider the equation

$$\left\{D^{n+1}-D^n-A\left[1+ma_0\frac{\exp(s_0\lambda)}{F(\lambda)}\cos\omega\lambda\right]\right\}F(\lambda)=0. \tag{A13}$$

We will show that the solution of Eq. (A13) is such that $F(\lambda)\rightarrow a_0\exp(s_0\lambda)$ in the steady state, provided the output modulation is small, thus giving a solution for an input of the form of Eq. (A12).

Equation (A13) may be solved by Laplace transformation to give

$$F(\lambda)=a_0\exp(s_0\lambda)\{1+Am\cos(\omega\lambda-\Phi)\times[R^2+A^2-2AR\cos\phi]^{-\frac{1}{2}}\}, \tag{A15}$$

where a_0 is defined by Eq. (A11) and

$$R^2=(s_0^2+\omega^2)^n[(s_0-1)^2+\omega^2]$$
$$\phi=n\tan^{-1}(\omega/s_0)+\tan^{-1}[\omega/(s_0-1)]$$
$$\Phi=\tan^{-1}[(R\sin\phi)/(R\cos\phi-A)].$$

Let

$$\delta=A\omega m[R^2+A^2-2AR\cos\phi]^{-\frac{1}{2}}.$$

Then

$$F(\lambda)\rightarrow a_0\exp(s_0\lambda)[1+(\delta/\omega)\cos(\omega\lambda-\Phi)],\ \lambda\rightarrow\infty.$$

Hence

$$v_n(\lambda)\rightarrow(s_0-1)-\frac{\delta\sin(\omega\lambda-\Phi)}{1+(\delta/\omega)\cos(\omega\lambda-\Phi)}. \tag{A16}$$

If now $(\delta/\omega)\ll1$, the output modulation is small and

$$v_n(\lambda)=s_0-1-\delta\sin(\omega\lambda-\Phi),$$

with $v_0(\lambda)$ given by Eq. (A12).

Feedforward Filter

The equations governing this stage are Eqs. (3a) and (3b). The steady-state solution is

$$v_0'(\infty)=v_0(\infty)$$
$$v_1(\infty)=v_0/[1+v_0(\infty)].$$

To find the output when the input is $v_0(\infty)+\beta f(\lambda)$, where β is a small positive number, we may use standard perturbation technique. Thus, we let

$$v_1(\lambda)=v_1(\infty)+\beta g(\lambda)+\cdots \tag{A17}$$

$$v_0'(\lambda)=v_0(\infty)+\beta h(\lambda)+\cdots. \tag{A18}$$

Equations (A17) and (A18) when substituted into Eqs. (3) give, to first order in β,

$$Dg(\lambda)+[1+v_0(\infty)]g(\lambda)=f(\lambda)-v_1(\infty)h(\lambda) \tag{A19}$$

$$(\tau_D/\tau_F)Dh(\lambda)+h(\lambda)=f(\lambda), \tag{A20}$$

which are linear equations. Equation (A20) represents a linear RC integrator (time constant τ_D/τ_F) whose input is $f(\lambda)$ and whose output is $h(\lambda)$. The solution for $h(\lambda)$ may be substituted in Eq. (A19). The right side of Eq. (A19) is then known and represents the input to another RC integrator {time constant $1/[1+v_0(\infty)]$} whose output is $g(\lambda)$.